



## Calcium drives fusion of SNARE-apposed bilayers

Aleksandar Jeremic, Marie Kelly, Jin Ah Cho, Sang-Joon Cho, J.K. Heinrich Horber, Bhanu P. Jena\*

*Department of Physiology, Wayne State University School of Medicine, 5239 Scott Hall, 540 E. Canfield Avenue, Detroit, MI 48201, USA*

Received 17 October 2003

### Abstract

*N*-ethylmaleimide-sensitive factor attachment protein receptor (SNARE) has been proposed to play a critical role in the membrane fusion process. The SNARE complex was suggested to be the minimal fusion machinery. However, there is mounting evidence for a major role of calcium in membrane fusion. Hence, the role of calcium in SNARE-induced membrane fusion was the focus of this study. It revealed that recombinant v-SNARE and t-SNARE, reconstituted into separate liposomes, interact to bring lipid vesicles into close proximity, enabling calcium to drive fusion of opposing bilayers. Exposure to calcium triggered vesicle fusion at both, high potency and efficacy. The half-time for calcium-induced fusion of SNARE-reconstituted vesicles was determined to be ~10 s, which is two orders of magnitude faster than in its absence. Calcium acts downstream of SNAREs, since the presence of SNAREs in bilayers increases the potency of calcium-induced vesicle fusion, without significantly influencing its efficacy. Hence, this study suggests that in the physiological state in cells, both SNAREs and calcium operate as the minimal fusion machinery.

© 2003 Published by Elsevier Ltd.

**Keywords:** Calcium; Membrane fusion; SNAREs

### 1. Introduction

Exocytosis is a fundamental cellular process governing important physiological functions like enzyme secretion, and the release of hormones and neurotransmitters. This process involves fusion of membrane-bounded secretory vesicle at the base of plasma membrane-associated porosomes or fusion pores (Jena et al., 2002; Jeremic et al., 2003) and the expulsion of vesicular contents. Fusion of membrane-bounded secretory vesicles with the target membrane of the Porosome is a highly regulated event, where a large number of proteins participate. Among them, the soluble *N*-ethylmaleimide-sensitive factor attachment protein receptors (SNAREs), t-SNARE or target SNARE (syntaxin, SNAP-25/23) at the Porosome membrane (Jena et al., 2002) and secretory vesicle associated SNARE or v-SNARE (synaptobrevin or VAMP) has been proposed to be the minimal fusion machinery (Weber et al., 1998).

Cleavage of SNAREs by clostridial toxins has been known to block neurotransmission (Jahn and Niemann, 1994). Studies, however, report calcium ( $\text{Ca}^{2+}$ ) to be the major fusogen, whereas SNAREs promote  $\text{Ca}^{2+}$  sensitivity to the fusion process (Coorssen et al., 1998; Tahara et al., 1998; Zimmerberg et al., 2000). Studies further reveal that micro domains of high  $\text{Ca}^{2+}$  concentrations co-localize at the fusion site (Llinas et al., 1992a,b).  $\text{Ca}^{2+}$  ion channels have been found to associate with the SNARE complex (Sheng et al., 1996) and also with the porosome or fusion pore (Jena et al., 2002; Jeremic et al., 2003). Furthermore, in the presence of  $\text{Ca}^{2+}$ , t-SNAREs and v-SNARE in opposing bilayers interact in a circular array to form conducting pores (Cho et al., 2002d). Finally, several  $\text{Ca}^{2+}$ -binding proteins such as synaptotagmin and syncollin, which interact with SNAREs in a  $\text{Ca}^{2+}$ -dependent manner, have also been identified (Edwardson et al., 1997; Sudhof and Rizo, 1996) further supporting the involvement of  $\text{Ca}^{2+}$ . Hence, there is growing evidence supporting  $\text{Ca}^{2+}$  as a key player in membrane fusion. To determine the role of  $\text{Ca}^{2+}$  in SNARE-induced membrane fusion, the fusion of t-/v-SNARE-reconstituted

\* Corresponding author. Tel.: +1-313-577-1532; fax: +1-313-993-4177

E-mail address: bjena@med.wayne.edu (B.P. Jena).

liposomes was investigated using 6 different approaches. Results from all of them lead to the same conclusion: (i) a low fusion rate ( $\tau=16$  min) between t- and v-SNARE-reconstituted liposomes in the absence of  $\text{Ca}^{2+}$ ; and (ii) exposure of t-/v-SNARE liposomes to  $\text{Ca}^{2+}$ , drives vesicle fusion on a physiological relevant time-scale ( $\tau \sim 10$  s), demonstrating an essential role of  $\text{Ca}^{2+}$  in membrane fusion. This study also confirms earlier findings on the role of  $\text{Ca}^{2+}$  and SNAREs in cortical vesicle fusion in sea urchin eggs (Coorssen et al., 1998; Zimmerberg et al., 2000), where  $\text{Ca}^{2+}$  acts downstream of SNAREs., since the  $\text{Ca}^{2+}$ -effect on membrane fusion in SNARE-reconstituted liposomes is downstream of SNAREs, this suggests that the role of  $\text{Ca}^{2+}$ -binding proteins is regulatory in the physiological state.

## 2. Materials and methods

### 2.1. Preparation of liposomes

All lipids were obtained from Avanti Polar Lipids (Alabaster, AL). A 10-mM lipid stock solution was prepared by mixing lipid solution in chloroform- DOPC (1,2-dioleoyl phosphatidylcholine): DOPS (1,2-dioleoyl phosphatidylserine) in 70:30 by weight ratios in glass test tubes. The lipid mixture was dried under a gentle stream of nitrogen and resuspended in decane. The lipids were suspended in buffer containing 10 mM Hepes-NaOH [pH=7.5] and 140 mM NaCl or 150 mM KCl by vortexing for 5 min at room temperature. Large unilamellar vesicles (LUV) were formed following sonication for 2 min. Typically, vesicles of 0.2–2  $\mu\text{m}$  in diameter range were obtained as assessed by light and atomic force microscopy. Additionally two sets of proteoliposomes were prepared by gently mixing t-SNARE complex (Syntaxin-1/SNAP-25; final concentration 5  $\mu\text{g}/\text{ml}$ ) or VAMP2-His<sub>6</sub> (final concentration 2.5  $\mu\text{g}/\text{ml}$ ) with the liposomes (Cho et al., 2002d), followed by three freeze/thaw cycles to enhance protein reconstitution at the vesicles membrane. Vesicles with uniform size were prepared by published extrusion method (MacDonald et al., 1991). 17 passes of a liposomal solution through a polycarbonate membrane using LiposoFast extruder (Avestin, Ottawa) were sufficient to produce liposomes of 100 nm in diameter.

### 2.2. Wide-angle X-ray diffraction studies

Ten microliter of a 10 mM lipid vesicle suspension was placed at the center of an X-ray polycarbonate film mounted on an aluminum sample holder, which was placed in a Rigaku RU2000 rotating anode X-ray diffractometer equipped with automatic data collection unit (DATASCAN) and processing software (JADE). Similarly, X-ray diffraction studies were also performed using t- and v-SNARE reconstituted liposomes both

in the presence and absence of  $\text{Ca}^{2+}$ . Experiments were performed at 25 °C. Samples were scanned with a rotating anode, using the nickel-filtered Cu K $\alpha$  line ( $\lambda=1.5418$  Å) operating at 40 kV and 150 mA. Diffraction patterns were recorded digitally with scan rate of 3°/min using a scintillation counter detector. The scattered X-ray intensities were evaluated as a function of scattering angle  $2\theta$  and converted into Å units, using the formula  $d$  (Å) =  $\lambda/2\sin\theta$ .

### 2.3. Light microscopy

Similar to X-ray diffraction studies, liposomes alone and SNARE-incorporated liposomes in the presence and absence of 5 mM  $\text{Ca}^{2+}$  were placed on glass cover slip and examined using transmitted-light in a bright field Axiovert 200 Zeiss microscope equipped with 40 $\times$  and 100 $\times$  objectives. Pictures were taken using an AxioCam digital camera (Carl Zeiss Inc., NY, USA) during the 30 min examination period.

### 2.4. Light scattering measurements

Vesicles aggregation and fusion was monitored using light scattering with excitation and emission wavelength set at 600 nm in a Hitachi F-2000 spectrophotometer (Wilschut et al., 1980). Seven microliters of vesicle suspension were injected into cuvettes containing 700  $\mu\text{l}$  of assay buffer (at 100  $\mu\text{M}$ , 37 °C).  $\text{Ca}^{2+}$  was included when appropriate. Light scattering was monitored for 5 min after injection of liposomes. Values are expressed in arbitrary units and as percent light scattered over control ( $n=6$ ). Student's *t*-test was used for comparisons between groups with significance established at  $P<0.05$  (★).

### 2.5. Fluorescence-dequenching measurements of membrane fusion

Membrane fusion was assessed by fluorescence dequenching using a slight modification of our published procedure (Sattar et al., 2002). Briefly, fusion of the rhodamine-labeled membranes of donor vesicles with unlabeled membranes of acceptor vesicles results in dilution of the label and hence it's dequenching or increase in fluorescence (Chen et al., 1993). In the fusion assay, 500  $\mu\text{l}$  of a 5 mM lipid vesicle suspension containing ~2% (mol) of octadecyl rhodamine (R-18) dye was prepared. In a typical fusion assay, 4  $\mu\text{l}$  unlabeled plain vesicles (AV) or v-SNARE-reconstituted vesicles were injected into a magnetically stirred cuvette containing 800  $\mu\text{l}$  of assay buffer, 40  $\mu\text{l}$  of R-18 labeled vesicles (AV or t-SNARE-reconstituted vesicles), in the presence and absence of  $\text{Ca}^{2+}$ . Fluorescence was measured continuously using a Hitachi F-2000 spectrophotometer at 560 nm excitation and 590 nm emission wavelengths at 37 °C. The row fluorescence, corrected for dilution, was

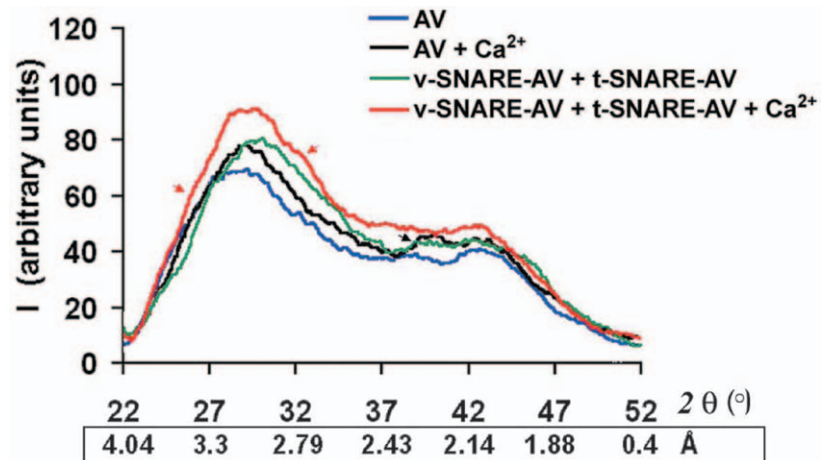


Fig. 1. Wide-angle X-ray diffraction patterns of interacting lipid vesicles. Representative diffraction profiles from one of four separate experiments using plain and t- and v-SNARE-reconstituted lipid vesicles, both in the presence or absence of 5 mM  $\text{Ca}^{2+}$  is shown. Note the shift of major (3.1 Å) peak toward smaller distances, when t-SNARE and v-SNARE-reconstituted vesicles interact. Arrows mark appearance of new peaks in X-ray diffractograms.

converted into a percentage of the total fluorescence after addition of Triton X-100 (0.5% v/v) at the end of each experiment, representing 100% of total fluorescence. The initial fluorescence of labeled vesicles, before addition of unlabeled vesicles, was then taken as 0% of total fluorescence. Data have been expressed as mean  $\pm$  SEM of 5 separate experiments. Student's *t*-test was used for comparisons between groups with significance established at  $P < 0.05$  (★).

## 2.6. Electrophysiological bilayer setup

Electrical measurements of the artificial lipid membrane were performed using a bilayers setup (Cho et al., 2002d). Capacitance and conductance versus time were recorded using pulse software, an EPC9 amplifier and probe from HEKA (Lambrecht, Germany). Membranes were formed while being held at 0 mV. A baseline current was established prior to the addition of SNARE and SNARE-vesicles. t-SNARE-reconstituted vesicles containing nystatin and the cholesterol homologue ergosterol were added to the cis-side of the chamber containing v-SNARE in the bilayer membrane and capacitance and conductance monitored. When vesicles containing nystatin were incorporated into the bilayer, a current spike could be detected (Cho et al., 2002d). Experiments were performed in the presence and absence of 1 mM  $\text{CaCl}_2$  and 5 mM EGTA.

## 2.7. Atomic force microscopy

Membrane fusion was assessed using atomic force microscopy (AFM) (Cho et al., 2002a,b,c,d; Schneider et al., 1997). t-SNARE-associated vesicles in buffer were attached to a freshly cleaved mica surface. v-SNARE-associated liposomes then were added to the attached

t-SNARE vesicles. The t-/v-SNARE-associated vesicles were monitored using the AFM for several min (up to 30 min) followed by addition of  $\text{Ca}^{2+}$ . The effect of  $\text{Ca}^{2+}$  on the t-v-SNARE-associated liposomes was further examined in the AFM for 10–15 min. Section analysis of vesicle size change was determined throughout the study. Imaging of phospholipid vesicles was performed using Nanoscope IIIa (Digital Instruments, Santa Barbara, CA, USA). Vesicles were imaged using “tapping” mode in fluid with Oxide-sharpened silicon nitride contact mode cantilevers, with a spring constant of 0.38  $\text{N}\cdot\text{m}^{-1}$  and an imaging force of  $< 200$  pN. To increase the force sensitivity, an ActivResonance Controller (Infinitesima, Bristol, UK) was used. The cantilever was driven at frequencies around 2 kHz. Images were obtained at line frequencies of 2 Hz, with 512 lines per image, and constant image gains. Topographical dimensions of liposomes were analyzed using the software nanoscopeIIIa.4.3r8 supplied by Digital Instruments.

## 3. Results

### 3.1. Interaction(s) between t- and v-SNARE-reconstituted liposomes revealed by X-ray diffraction

X-ray diffraction patterns of non-reconstituted (plain) vesicles and t- and v-SNARE-reconstituted vesicles in the absence and presence  $\text{Ca}^{2+}$  are shown in Fig. 1. To our knowledge, these are the first recorded wide-angle diffractograms of unilamellar (single bilayer) vesicles in solution in the 2–4 Å diffraction range. A broad diffraction pattern is demonstrated, spanning  $2\theta$  ranges approximately 23–48° or *d* values of 1.9–3.9 Å with sharp drop-off intensity on either sides of the range.

Table 1

Short-range interactions between lipid bilayers measured by X-ray diffraction. Data represents mean  $\pm$  SEM of four separate experiments

Sample	Imax	Imax	(Å)
	(a.u.)	(2 $\theta$ )	
AV	64 $\pm$ 4	28.5 $^{\circ}$ $\pm$ 0.1	3.1
AV+Ca <sup>2+</sup>	84 $\pm$ 6	29.4 $^{\circ}$ $\pm$ 0.1	3.0
AV-t-/v-SNARE	86 $\pm$ 5	30.5 $^{\circ}$ $\pm$ 0.1	2.9
AV-t-/v-SNARE+Ca <sup>2+</sup>	98 $\pm$ 4	29.5 $^{\circ}$ $\pm$ 0.2	3.0

The scattering curve exhibits a diffuse, asymmetric diffraction pattern typical of the short-range ordering in a liquid system, and indicating a multitude of contacts between interacting vesicles with characteristic lengths of 1.9–3.9 Å. Dehydrated or partially hydrated liposomes, however, were unable to interact in such a way, and therefore failed to yield any patterned diffractograms (data not shown). Hence, only fully hydrated liposomes in solution have the freedom to interact with each other, and diffract as shown (Fig. 1). This suggests that water is a key molecule in such interactions, resulting in such ordered diffracting patterns.

Two broad peaks are visible on the diffractogram, the stronger at 3.1 Å and a weaker at 2.1 Å (Fig. 1). They indicate that the majority of the contacts between vesicles have such characteristic lengths. Below 2 Å, X-ray diffraction signals disappear rapidly leading to the conclusion that the observed characteristic lengths are due to layer formation at the contact area between vesicles. High repulsive hydration and electrostatic forces, prevents further approach of the lipid bilayers below 2 Å (Huster et al., 1999; McIntosh, 2000). The addition of Ca<sup>2+</sup> or incorporation of SNAREs at the vesicles membrane or both influences both peaks within the 2.1–3.3 Å intensity range (Fig. 1). The influence of Ca<sup>2+</sup> and SNAREs or both is observed more pronounced on the peak positioned at 3.1 Å, where an increase in peak intensity (Imax), symmetry and a shift in peak position are detectable (Fig. 1; Table 1). Furthermore, a new peak arises at 2.3 Å upon addition of Ca<sup>2+</sup> to liposomes (depicted by black arrow, Fig. 1), and may represent Ca-O bond formed between Ca<sup>2+</sup> ions and phosphate lipid head groups. Analogous to this X-ray study, a Ca-O bond length of approximately 2.5 Å was reported for dicalcium phosphate salts (Beever, 1958) and Ca<sup>2+</sup>-lipid complexes (Laroche et al., 1991). Incorporation of the t- and v-SNARE proteins at the vesicle membrane stabilize inter-vesicular interactions, to bring vesicles closer as demonstrated by an increase in intensity of the major (3.1 Å) peak and Imax shift from 3.1 Å to 2.9 Å (Table 1). Addition of Ca<sup>2+</sup> to the t-/v-SNARE-associated liposomes yields the largest increase in the peak intensity with additional contributions on both sides of the 3.1 Å peak, at 2.8 Å and

3.4 Å, respectively (depicted by red arrows, Fig. 1) indicating a greater number of contacts between vesicles with exactly defined distances. Unlike t-/v-SNARE vesicles, interactions between t-/t-SNARE or v-/v-SNARE vesicles do not lead to stable vesicle contacts in solution, and hence liposome suspensions containing either t- or v-SNAREs exhibits little or no effect on the X-ray scattering patterns (data not shown). As discussed above, only with a mixture of t-SNARE and v-SNARE reconstituted-vesicles, a significant change in the X-ray diffraction patterns was observed (Fig. 1). Since Ca<sup>2+</sup> and SNAREs induce rearrangement and close apposition of the lipid vesicles in solution, both were further tested for their ability to promote membrane fusion. The effect of Ca<sup>2+</sup> on aggregation and/or fusion of plain and t-/v-SNARE-reconstituted vesicles were further examined using light scattering, light microscopy, atomic force microscopy (AFM), fluorescent dequenching and electrochemical measurements.

### 3.2. Vesicle aggregation and fusion observed by light scattering measurements and light microscopy

Ca<sup>2+</sup>- induced vesicles aggregation and fusion was determined using light scattering measurements (Wilschut et al., 1980). It is well known that light scattering properties mainly depend on the concentration (number) of the scattering particles in solution and to a lesser extent on the particle size. Thus, we utilized this experimental approach to monitor changes in the number of plain and SNARE-reconstituted vesicles in solution, both in the presence and absence of Ca<sup>2+</sup> (Fig. 2). Addition of Ca<sup>2+</sup>, induced a dose-dependent (5–20 mM) aggregation and fusion of plain vesicles, represented by the biphasic scattering curve (Fig. 2A). The initial rapid increase in intensity of light scattering was initiated by the addition of vesicles into the cuvette, followed by a slow decay of light scattering (Fig. 2A and B), representing interactions between vesicles in solution. In experiments where assay buffer was supplemented with milimolar Ca<sup>2+</sup>, a significant decrease in the light scattering was observed due to aggregation and fusion, leading to the settling of large vesicles as previously reported (Wilschut et al., 1980). Clearing of the light path due to vesicle settling occurs even in continually stirred reaction mixtures (data not shown). These results are further confirmed by light microscopy, demonstrating aggregation and fusion of plain lipid vesicles upon addition of Ca<sup>2+</sup> (data not shown). In the absence of Ca<sup>2+</sup>, SNAREs failed to induce any significant aggregation and fusion of vesicles, since the plain and t-/v-SNARE-associated vesicles exhibited similar light scattering patterns (Fig. 2A and B). Thus, in the absence of Ca<sup>2+</sup>, no significant change in the number and size of proteoliposomes is observed, compared to plain (control) vesicles. This was further



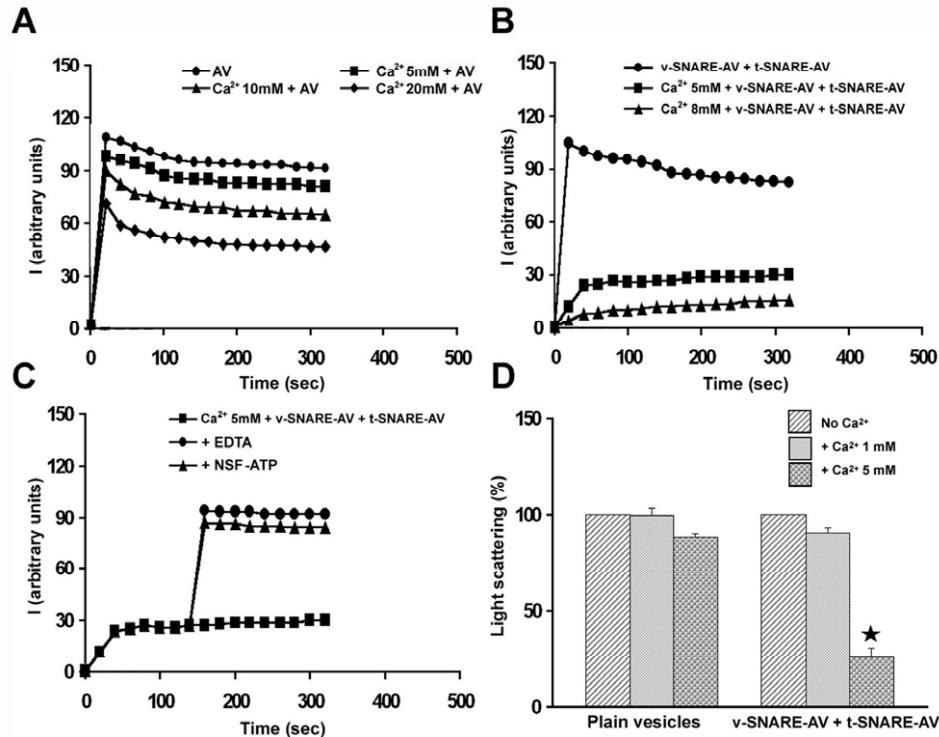


Fig. 2. Light scattering profiles of plain and SNARE-associated vesicles.  $\text{Ca}^{2+}$ -induced aggregation and fusion of plain liposomes is dose dependent (A). SNARE-associated vesicles exhibit the same scattering pattern as plain lipid vesicles. Addition of 5 mM  $\text{Ca}^{2+}$  drives SNAREs vesicle fusion, resulting in fewer vesicles and consequently a 4-fold decrease in light scattering intensity (B). Addition of *NSF*-ATP (1  $\mu\text{g}/\text{ml}$ ) or EDTA (5 mM), however, prevents vesicle aggregation and fusion (C). Presence of the t/v-SNARE in bilayers potentiate the effect of 5 mM  $\text{Ca}^{2+}$  ( $\star P < 0.05$ , Student *t*-test between plain and SNARE vesicles,  $n=6$ ) and furthermore, lower the  $\text{Ca}^{2+}$  requirement for fusion to 1 mM (D).

confirmed by light microscopy studies (Fig. 3). Light microscopy shows that t-SNARE and v-SNARE vesicles in solution interact to produce vesicle dimers, which remain firmly connected to each other, even after a 30-min period (Fig. 3A). Previous studies (Fasshauer et al., 1998; Jeong et al., 1998; Poirier et al., 1998) reported the stability and tight interaction between the t/v-SNARE proteins. A suspension containing either the t-t-SNARE or v-v-SNARE vesicles, lack such ability to form dimers (data not shown).

In the presence of  $\text{Ca}^{2+}$  (5–8 mM), t- and v-SNARE-associated vesicles exhibit an almost 4-fold reduction in intensity of light scattering (Fig. 2B). Loss in light scattering is a consequence of vesicle fusion, resulting in increase of vesicle size and decrease in vesicle number. In conformation, light microscopy studies demonstrate an increase in proteoliposome size following addition of 5 mM  $\text{Ca}^{2+}$  to the t/v-SNARE vesicles suspension (Fig. 3). The increase in proteoliposome size in the presence of  $\text{Ca}^{2+}$  was more pronounced in case of smaller (100 nm) vesicles (Fig. 3C and D) compared to micrometer size vesicles (Fig. 3A and B). Although the 100 nm vesicles are below the detection limit of the light microscope (Fig. 3C), addition of  $\text{Ca}^{2+}$  triggers membrane fusion, resulting in the production of larger and visible vesicles (Fig. 3D).

Earlier studies (Ohki, 1984; Wilschut et al., 1981) also reported a size dependence on vesicle fusion. Vesicle fusion has been found to be inversely proportional to vesicle diameter. Hence, as diameter of vesicles increase, vesicle fusion decreases (Ohki, 1984).

When EDTA or *NSF*-ATP (*NSF*-ATP disassembles the t/v-SNARE complex; Hanson et al., 1997) were added to the assay mixture containing t- and v-SNARE vesicles and 5 mM  $\text{Ca}^{2+}$ , our light scattering studies demonstrate a significant inhibition in aggregation and fusion of proteoliposomes (Fig. 2C). This result further supports  $\text{Ca}^{2+}$  to be a trigger in fusion of SNARE-associated vesicles. *NSF*, in the absence of ATP, did not have any significant effect on the light scattering properties (data not shown). These results support the view that *NSF*-ATP disassembles the SNARE complex, thereby reducing the number of interacting vesicles in solution. Similarly, addition of EDTA chelates free  $\text{Ca}^{2+}$  and prevents fusion of SNARE-associated vesicles (Fig. 2C). These studies further demonstrate that  $\text{Ca}^{2+}$ -driven vesicle fusion is SNARE-sensitive since reconstitution of SNARE proteins at the vesicles membrane lowers the  $\text{Ca}^{2+}$  requirement for vesicle fusion (Fig. 2D). Results from these studies demonstrate that while SNAREs bring vesicles in close apposition,  $\text{Ca}^{2+}$  triggers fusion between them.

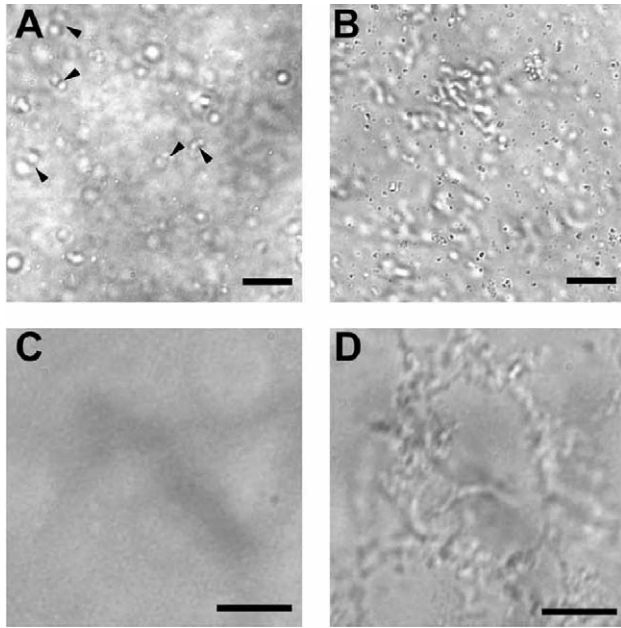


Fig. 3. Light microscopy demonstrates  $\text{Ca}^{2+}$ -induced aggregation and fusion of SNARE-associated vesicles. t- and v-SNARE-associated vesicles dimerize but fail to fuse in the absence of  $\text{Ca}^{2+}$ . Arrowheads mark representative examples of long-lasting (30 min) vesicle dimers brought together by SNAREs (A). Only following addition of  $\text{Ca}^{2+}$  (5 mM), an aggregation and fusion of SNAREs vesicles is demonstrated (B). To better assess changes in proteoliposomes size, hidden under the broad size distribution of starting vesicles, SNARE vesicles were first uniformly sized to 100 nm by extrusion method (C) and then incubated with 5 mM  $\text{Ca}^{2+}$  (D). Note no vesicles are visible due to the resolution limit of the light microscope (C). However, as early as 2 s following addition of  $\text{Ca}^{2+}$  to the SNARE-reconstituted liposomal suspension, a marked increase in proteoliposomes size due to fusion and coalescing of vesicles is demonstrated (D). Scale bar 10  $\mu\text{m}$ .

### 3.3. Membrane fusion examined using fluorimetric fusion assay

Fluorimetric membrane fusion assays were performed using published procedures (Sattar et al., 2002) (Fig. 4). Fluorimetric membrane fusion assays also reveal that in the absence of  $\text{Ca}^{2+}$ , there is loss in efficiency of fusion between t- and v-SNARE vesicles (Fig. 4A and B). Minimal change in fluorescence obtained during collisions of plain (control) vesicles (AV+AV) demonstrates that nonspecific dye transfer is negligible (Fig. 4A). In the presence of  $\text{Ca}^{2+}$ , however, the potency and efficacy of fusion of plain and t-/v-SNARE vesicles was greatly increased. Addition of 5 mM  $\text{Ca}^{2+}$  to the liposomes solution, elicited a 5-fold increase in fluorescence (Fig. 4A), which is comparable to the observed decrease in light scattering as a consequent loss in vesicle number following fusion (Fig. 3B). The presence of SNAREs in bilayers increased the sensitivity of  $\text{Ca}^{2+}$  on vesicles fusion, since reconstitution of SNARE proteins at the vesicles membrane lowers the  $\text{Ca}^{2+}$  requirement for

vesicle fusion (data not shown) and potentiates the effect of 5 mM  $\text{Ca}^{2+}$  (Fig. 4A).

In the presence of  $\text{Ca}^{2+}$ , the rate and amount of membrane fusion for the first 10 s is similar for plain and SNARE-associated vesicles (Fig. 4A). However, a significant influence of SNAREs on the total amount of  $\text{Ca}^{2+}$ -induced fusion is observed at longer times (Fig. 4A). This potentiation of  $\text{Ca}^{2+}$ -induced vesicle fusion may be due to the increase in number of interacting vesicles in solution in the presence of both  $\text{Ca}^{2+}$  and SNAREs (Figs. 2 and 3). Alternatively, the free energy released from SNARE complex formation might be used to enhance lipid mixing, thus enabling  $\text{Ca}^{2+}$  to drive vesicle fusion more potently. The kinetics of vesicle fusion is first order (Fig. 4B). Vesicle fusion in the presence of t/v-SNAREs and  $\text{Ca}^{2+}$  proceeds with an initial rate constant of  $k=0.0911 \pm 0.0045 \text{ s}^{-1}$  corresponding to reaction half-time of  $\tau=7.6 \pm 0.6 \text{ s}$  during the first 25 s. In this initial period, which is about three reaction half-times, 87% of vesicle fusion is completed. The rest of the fusion proceeds at a somewhat lower rate, with  $k=0.0375 \pm 0.0015 \text{ s}^{-1}$  corresponding to reaction half-time of  $\tau=18.5 \pm 0.5 \text{ s}$  (Fig. 4B). Fusion of SNARE vesicles in the absence of  $\text{Ca}^{2+}$  proceeds much slower, with a rate constant of  $k=0.0007 \pm 0.00007 \text{ s}^{-1}$  corresponding to a reaction half-time of  $\tau=990 \pm 90 \text{ s}$ , which is approximately two orders of magnitude slower than in the presence of  $\text{Ca}^{2+}$  (Fig. 4B). In the absence of  $\text{Ca}^{2+}$ , the kinetics of SNARE-induced vesicle fusion obtained in our study ( $\tau=16 \text{ min}$ ) is comparable to the rates of fusion of SNARE-reconstituted vesicles ( $\tau=10\text{--}40 \text{ min}$ ) measured in previous studies (Parlati et al., 1999; Weber et al., 1998).

### 3.4. Electrochemical measurements of fusion of SNARE-apposed bilayers

Using electrophysiological measurements,  $\text{Ca}^{2+}$ -driven fusion of SNARE-apposed bilayers was examined. The capacitance and conductance of v-SNARE-reconstituted bilayers, in the presence and absence of t-SNARE-reconstituted vesicles and/or  $\text{Ca}^{2+}$ , was studied (Fig. 5) using a published procedure (Cho et al., 2002d; Jeremic et al., 2003). This experimental approach is more sensitive than the light scattering and lipid mixing assays, as it is capable of assessing membrane fusion on a single event scale. In the absence of  $\text{Ca}^{2+}$ , the t-SNARE-reconstituted vesicles failed to fuse with the v-SNARE-reconstituted bilayer during 5-min of recording. Hence, during these 5 min, no change in conductance and capacitance of the lipid membrane was detected (Fig. 5B). However, in the presence of 1 mM  $\text{Ca}^{2+}$ , t-SNARE vesicles fused with the v-SNARE bilayer, which could be detected by an abrupt increase in both conductance and capacitance of the v-SNARE-associated lipid membrane (Fig. 5C). Furthermore,

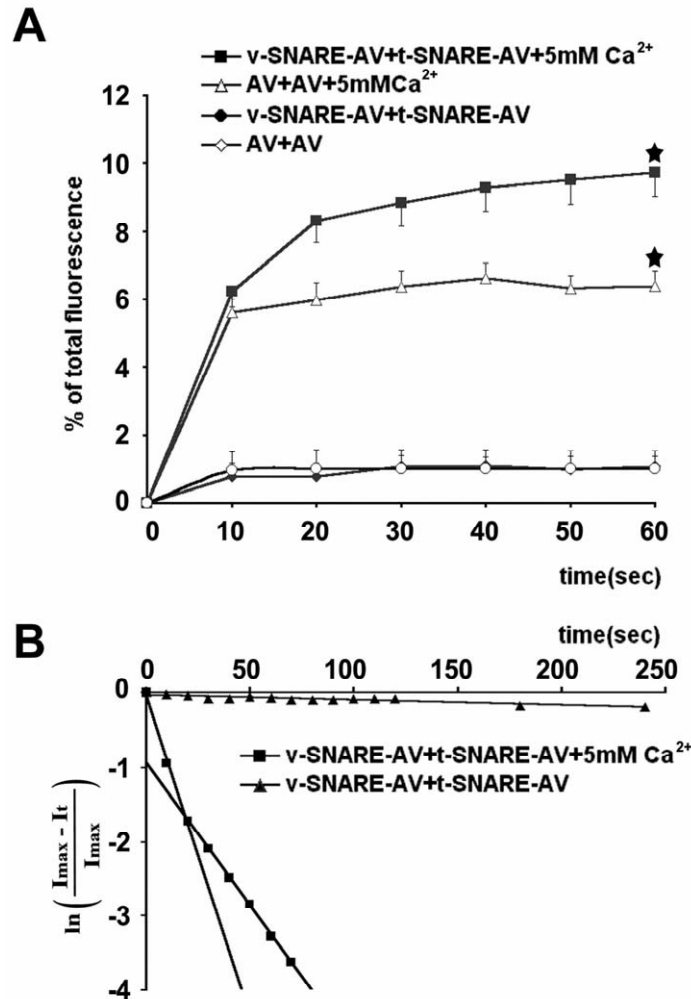


Fig. 4. Fluorimetric fusion assays demonstrate the ability of  $\text{Ca}^{2+}$  to induce rapid lipid mixing of plain (AV) and SNARE-associated vesicles. Addition of 5 mM  $\text{Ca}^{2+}$  to liposomal solution significantly increases the fusion of plain and SNARE-associated vesicles ( $\star P < 0.05$ , Student *t*-test between AV and AV+ $\text{Ca}^{2+}$  or t-/v-SNARE-AV+ $\text{Ca}^{2+}$ ,  $n=5$ ). Note the inability of SNAREs in the absence of  $\text{Ca}^{2+}$  to significantly induce vesicle fusion ( $P > 0.1$ , Student *t*-test between AV and t-/v-SNARE-AV,  $n=5$ ). Incorporation of t-/v-SNAREs at the vesicles membrane increases the overall yield but does not alter the rate of  $\text{Ca}^{2+}$ -induced membrane fusion (A). The graph depicts the first-order kinetics of SNAREs vesicle fusion in the presence and absence of  $\text{Ca}^{2+}$  (B).

$\text{Ca}^{2+}$ -requirement for membrane fusion using this sensitive method was determined to be  $\sim 100 \mu\text{M}$  (data not shown). Addition of 3 mM KCl drives osmotically the fusion of vesicles with the artificial bilayer, and was used to assess the integrity of the lipid bilayer at the completion of an experiment. In a large presence of  $\text{Ca}^{2+}$ , since the majority of t-SNARE-associated vesicles underwent fusion with the v-SNARE membrane, little increase in fusion was detected following addition of the 3 mM KCl (Fig. 5C). In the presence of EGTA, however, addition of 3 mM KCl resulted in fusion, demonstrating that docked, t-SNARE vesicles had failed to fuse with the v-SNARE-reconstituted membrane, within the 5-min period (Fig. 5B). Results of this study demonstrate that fusion and continuity between the t-/v-SNARE-apposed bilayers, in a physiological relevant time scale, is established only in the presence of  $\text{Ca}^{2+}$ .

### 3.5. Fusion of SNARE-apposed bilayers revealed by AFM

To confirm fusion between t- and v-SNARE vesicles, AFM was used as another technique able to analyze the process at the single vesicle level. The structure, arrangement and dynamics of t-/v-SNARE-associated vesicles demonstrated fusion of apposed t- and v-SNARE vesicles in the presence of  $\text{Ca}^{2+}$  (Fig. 6). This is the first direct visualization of t- and v-SNARE apposed vesicles fusing following the addition of  $\text{Ca}^{2+}$ . Hence, our studies suggest that SNAREs are involved in bringing vesicles in close proximity, enabling the  $\text{Ca}^{2+}$  to interact with the phospholipid head groups of the opposing bilayers to bring about fusion (Fig. 7). An actual pore formed by opposing v-SNAREs and t-SNAREs is depicted (blue arrow, Fig. 7). This pore is



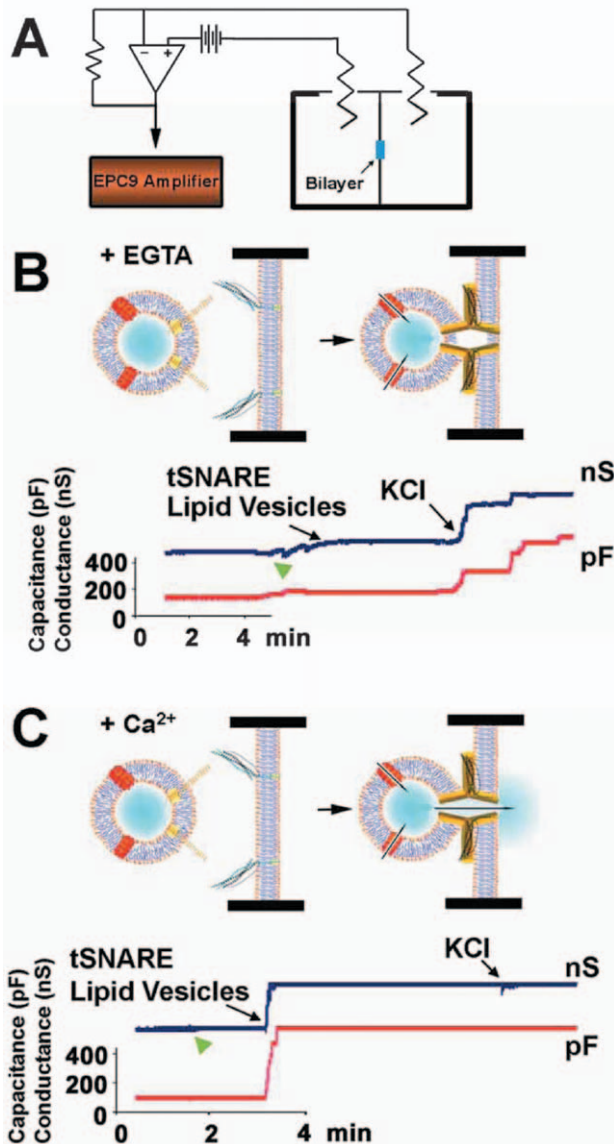


Fig. 5. Conductance and capacitance measurements of SNARE-reconstituted lipid bilayers. The EPC9-electrophysiological set up is shown (A). In the presence of 5 mM EGTA, t-SNARE-associated vesicles containing nystatin channels at their membrane (represented as red structures at the vesicle membrane) interact with v-SNARE-reconstituted lipid bilayer without fusing (B). Note no change in conductance or capacitance following exposure of SNARE-associated lipid vesicles to the bilayer. The vesicles fuse, however, when 3 mM KCl is applied, demonstrating fusion of docked vesicles and presence of an intact bilayer (B). The green arrowhead indicates when the stirring is switched on to mix the addition. In the presence of 1 mM  $\text{CaCl}_2$ , the t-SNARE-associated vesicles fuse with the v-SNARE-reconstituted bilayer as depicted in a consequent increase in conductance and capacitance. Since a large majority of docked vesicles have fused, addition of 3 mM KCl has no further effect (C). Traces (B–C) are representative profiles from one of five separate experiments.

rendered conductive in the presence of  $\text{Ca}^{2+}$  (Cho et al., 2002d), thus establishing continuity between the opposing vesicles.

#### 4. Discussion

The current hypothesis centers SNAREs as the key component in membrane fusion (Sollner et al., 1993). v- and t-SNAREs reconstituted into separate liposome populations initiate fusion of apposing vesicles (Parlati et al., 1999; Weber et al., 1998), albeit at a slow rate ( $\tau=10\text{--}40$  min). Our recent studies on the fusion pore or porosome complex (Jena et al., 2002; Jeremic et al., 2003) have demonstrated the association of a  $\text{Ca}^{2+}$  channel with the native porosome complex. Hence, the present study was aimed at evaluating the influence of  $\text{Ca}^{2+}$  on fusion of t-SNARE and v-SNARE-reconstituted vesicles. In the absence of  $\text{Ca}^{2+}$ , fusion between t- and v-SNARE vesicles proceeds at a very slow rate ( $\tau=16$  min) similar to values reported earlier (Parlati et al., 1999; Weber et al., 1998). Following addition of  $\text{Ca}^{2+}$ , however, SNARE-associated liposomes fuse rapidly, approaching physiological time-scales ( $\tau=7.6$  s), and demonstrating that  $\text{Ca}^{2+}$  is an essential component of the minimal fusion machinery.

Native and synthetic vesicles exhibit a significant negative surface charge primarily due to the polar phosphate head groups. These polar head groups produce a repulsive force, preventing aggregation and fusion of apposing vesicles. Collisions and subsequent repulsions of plain vesicles in solution as a result of Brownian motion and electrostatic interactions have been observed using light microscopy. Contact areas that are established between plain vesicles in suspension are random and transient (lasting seconds or less), and are revealed as broad intensity distributions in the X-ray diffractograms. In a number of earlier X-ray diffraction studies (Nagle and Tristram-Nagle, 2000), the low-angle scattering patterns of multilamellar vesicle suspensions exhibit several sharp reflections, corresponding to the lamellar repeat period of 66–67 Å, and thus indicating the presence of stacked bilayers separated by a fluid space. The wide-angle X-ray pattern exhibiting a single reflection centered at 4.6 or 4.18 Å, on other hand, is consistent with spacing between lipid chains found in a liquid or gel phase, respectively. In contrast to reports using multilamellar vesicles, we observed a diffuse and asymmetric X-ray diffraction pattern in the range of 2–4 Å in our unilamellar vesicle suspension. Furthermore, diffraction patterns could be observed only with fully hydrated vesicles. If water evaporates during running a diffractogram or if the sample is dehydrated, the signal collapses to zero.

These results lead to a conclusion that such diffraction patterns are generated, similar to observations with multilamellar vesicles, from the contact areas between apposing bilayers modulated by water. In support of this conclusion earlier experiments with osmotically squeezed hydrated bilayers, indicate the formation of an extremely narrow (2 Å) fluid space between bilayers



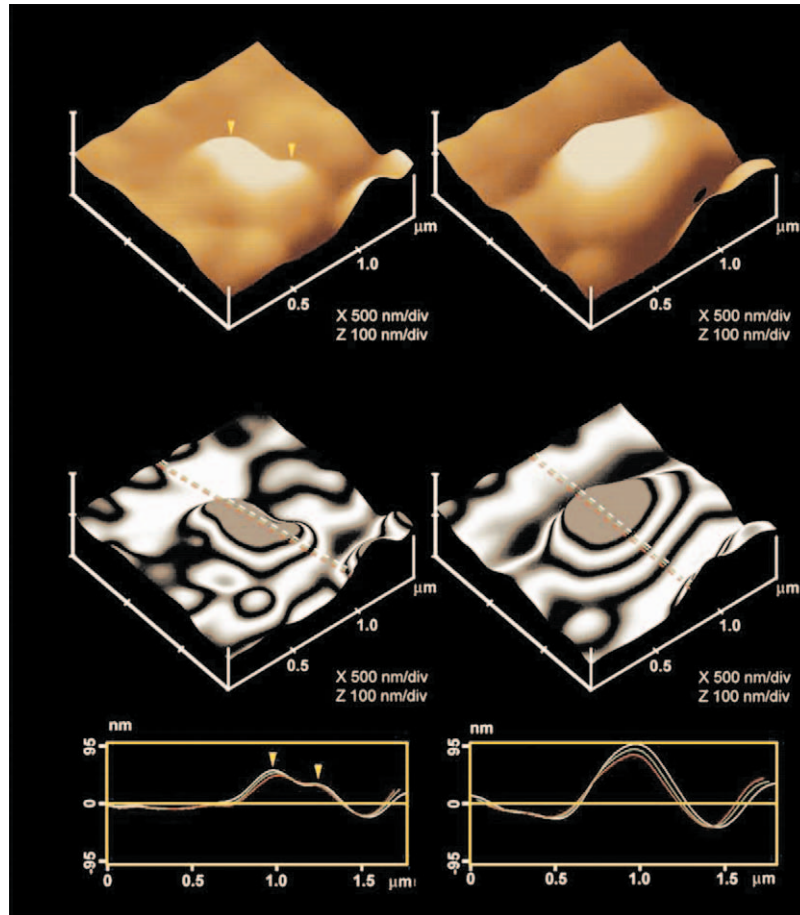


Fig. 6. Atomic Force Micrograph (AFM) depicting the fusion of two t- and v-SNARE-associated vesicles in the presence of 5 mM  $\text{Ca}^{2+}$ . Upper panel demonstrates 3-dimensional AFM micrograph before (Left) and after  $\text{Ca}^{2+}$  treatment (Right). Yellow arrowheads indicate the presence of the two vesicles. Lower panel shows the section analysis of the AFM micrograph demonstrating size difference before (Left) and after addition of  $\text{Ca}^{2+}$  (Right).

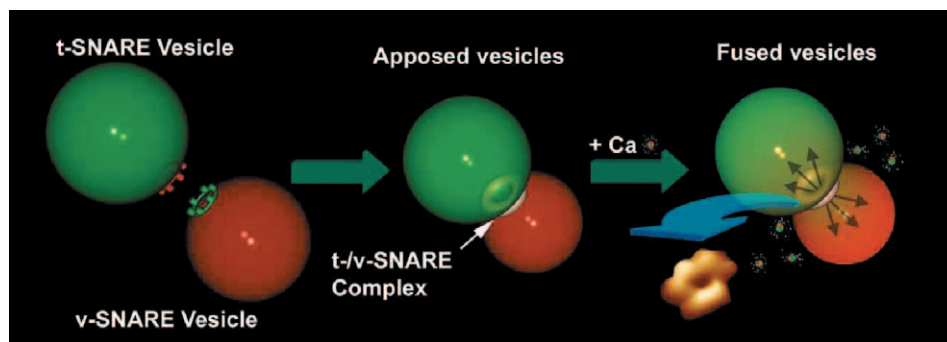


Fig. 7. The illustration depicts dimerization of t-SNARE and v-SNARE vesicles and the interaction of t-SNARE and v-SNARE in a circular array to form a conducting pore in the presence of  $\text{Ca}^{2+}$ . The blue arrow points to an AFM micrograph of actual pore formed when t- and v-SNAREs in apposing bilayers interact in circular array.

(Kulkarni et al., 1999). At this distance, strong repulsive forces are generated preventing further approach of bilayers, reflected by the sharp disappearance of signal below 2 Å in our diffractograms, and indicating the lack of intervesicular contacts. The possibility that X-ray diffractograms are in part generated through the

rearrangement and ordering of hydrocarbon chains in the lipid bilayers cannot be ruled out. Nevertheless, in the presence of  $\text{Ca}^{2+}$  or SNAREs, there is a significant increase in the intensity of the X-ray signal pointing to an increase in number and/or size of contact areas between apposing vesicles. This was confirmed by our

light and atomic force microscopy studies. Furthermore, additional X-ray intensity contributions are observed only in the presence of  $\text{Ca}^{2+}$  and/or SNAREs. This may be attributed to the preferential spatial orientation of t-SNARE and v-SNARE vesicles making contact within a distance defined by the  $\text{Ca}^{2+}$  radius, in accordance with the  $\text{Ca}^{2+}$ -bridging and ionic radius hypotheses of membrane fusion (as explained below). Taking all facts into account, these results suggest that the observed diffuse X-ray diffraction signal arises from intermolecular contacts between phosphate head groups of the apposing bilayers, presumably bridged by water. The hydrogen bond formation between apposing phosphate groups can span a distance of 2.1–4.2 Å, depending on how phosphate groups are packed and hence, orientated in space (Pauling and Corey, 1953). Therefore, an exact spatial orientation of phosphate head groups may be a necessary requirement for membrane fusion, which may best be achieved in SNARE-associated membranes, in the presence of  $\text{Ca}^{2+}$ .

Interactions between t- and v-SNARE vesicles in solution, however, exhibit different characteristics compared with the interactions between plain vesicles. Mixing t- and v-SNARE-associated vesicles usually produces long-lasting vesicle dimers (lasting 30 min and longer) but rarely trimers. In the absence of  $\text{Ca}^{2+}$ , such proteoliposomes suspensions lack large vesicle aggregates, and demonstrate low fusogenic ability. Our X-ray, AFM and light microscopy studies, all demonstrate that interaction between t- and v-SNAREs allows close apposition of vesicles to approximately 2.1 Å distance. A further decrease in distance between the apposing lipid bilayers is prevented due to high repulsive hydration forces, as well as electrostatic and steric interactions (McIntosh, 2000), all serving as barriers for vesicles to fuse. Supporting this view, our membrane fusion studies demonstrate either a lack of fusion between t- and v-SNARE associated vesicles in the absence of  $\text{Ca}^{2+}$ , or if proteoliposomes fusion does occur, it does so extremely slowly on a physiological irrelevant time-scale of  $\tau=16$  min. Addition of  $\text{Ca}^{2+}$  to the t-/v-SNARE proteoliposomes, however, results in membrane fusion on the time-scale of  $\tau \sim 10$  s. Hence,  $\text{Ca}^{2+}$  is rate determining in fusion of both plain and SNARE-associated vesicles. Since SNAREs had little influence on the overall rate of vesicles fusion in the presence of  $\text{Ca}^{2+}$ , this suggests SNARE participation is upstream while that of  $\text{Ca}^{2+}$  downstream in membrane fusion. It might therefore be proposed that the minimal fusion machinery comprises two distinct components: one mediated by SNAREs, which controls docking of vesicles, and the other mediated by  $\text{Ca}^{2+}$  acts as the fusogen. In other words, SNAREs increase the likelihood for vesicles to make distinct and appropriate intervesicular contact(s) in solution, thus allowing  $\text{Ca}^{2+}$  to drive the fusion reaction.

The physiological relevance of these results can be demonstrated by a calculation made possible by assuming the same rate for fusion of the native vesicles with the plasma membrane, which is the same as for  $\text{Ca}^{2+}$ -induced liposomes fusion, i.e.  $k=0.0911 \text{ s}^{-1}$ . With this in mind, the first 1% of vesicles from the cellular pool would fuse within 100 ms. On the same assumption, the time required for the fusion of the first vesicle with the plasma membrane, from a pool of 30,000 stored vesicles in case of a neuroendocrine cell (Parsons et al., 1995; Plattner et al., 1997), would require less than 0.4 ms. This is consistent with the fact that, under physiological conditions,  $\text{Ca}^{2+}$  entry into the synapse triggers vesicles fusion and secretion from the readily releasable pool with a delay of only 0.1–0.5 ms (Jahn and Sudhof, 1999). Hence, this simple calculation shows that  $\text{Ca}^{2+}$ -induced vesicle fusion observed in this study is achieved in a physiologically relevant time scale.

Our membrane fusion and X-ray diffraction studies demonstrate that addition of  $\text{Ca}^{2+}$  to the liposomes solution triggers fusion of the lipid vesicles separated by 2.1–3.1 Å distance, suggesting that a critical distance is required between apposing bilayers to be able to fuse. The ionic radius of  $\text{Ca}^{2+}$  depends on its coordination number and lies between 1.1–1.5 Å (Shannon, 1976), which corresponds precisely to the observed distance between vesicles, where  $\text{Ca}^{2+}$  is effective (Fig. 1). The operating range of  $\text{Ca}^{2+}$  exactly matches these distances, and thus fits between apposing bilayers, bridging adjacent phosphate head groups, as proposed by Papahadjopoulos and co-workers (Portis et al., 1979). Indeed, infrared and Raman spectroscopy studies provide strong evidence that  $\text{Ca}^{2+}$  ions form bridges between phosphate groups of adjacent bilayers (Laroche et al., 1991). In agreement with the  $\text{Ca}^{2+}$ -bridging hypothesis, divalent cations ( $\text{Mn}^{2+}$ ,  $\text{Cd}^{2+}$  and  $\text{Sr}^{2+}$ ) with ionic radii similar to that of  $\text{Ca}^{2+}$  were able to activate the fast component of fusion, a selectivity that appears to be based on ionic radius (Kishimoto et al., 2001). It is tempting to speculate that the effect of  $\text{Ca}^{2+}$  and SNAREs may reflect their ability to span apposing membranes, acquiring a preferable membrane orientation required for fusion. Since the radius of  $\text{Ca}^{2+}$  action is limited to distances of 2–3 Å, obviously it requires some additional help from SNAREs to bring vesicles within this distance. Interaction of v- and t-SNAREs between opposing bilayers results in the formation of a SNARE complex in a circular array of a few nanometers in diameter (Fig. 7), hence besides defining the site of fusion, the t-/v-SNARE complex formed restricts and limits the fused space.

Other effects induced by  $\text{Ca}^{2+}$  and SNAREs in membrane fusion such as membrane phase or surface tension changes also may play a role. For example,  $\text{Ca}^{2+}$ -induced fusion of PS vesicles depends on the ability of  $\text{Ca}^{2+}$  to form an anhydrous complex between opposing

bilayers essentially free of interlamellar water (Wilschut et al., 1981). Alternately, the cause of  $\text{Ca}^{2+}$ -induced membrane fusion of PS membranes may lie in its ability to increase the surface tension of the membrane (Ohki, 1982).  $\text{Ca}^{2+}$  has also been found to induce phase changes in PS membranes, which results in tightly packed, highly ordered and a less hydrated membrane structure (Newton et al., 1978). Furthermore, our recent study supports the role of charged components in membrane fusion (Boinipally and Jena, unpublished observation). Native and synthetic vesicles exhibit high negative zeta potential in solution ( $-20$  to  $-30$  mV) that acts as a barrier for vesicles to fuse. Our study has also demonstrated that addition of SNAREs were unable to neutralize negative surface charges at the vesicle membrane. In contrast,  $\text{Ca}^{2+}$  abolished repulsive forces between the vesicles by its interaction with negative surface charges and thus increasing the chance for fusion. Finally, extremely high chemical affinity of  $\text{Ca}^{2+}$  toward phosphate and its hydration properties make  $\text{Ca}^{2+}$  ideal for membrane fusion, compared to other divalent cations of similar charge and radius.

In this study, using a cell-free system of plain and SNARE-reconstituted liposomes, we assessed the contribution of  $\text{Ca}^{2+}$  and SNAREs in membrane fusion. The fusion events required  $\text{Ca}^{2+}$ , at concentrations  $100\text{ }\mu\text{M}$  and higher. Although the actual  $\text{Ca}^{2+}$  concentration at the release site during a stimulus is not known, the opening of  $\text{Ca}^{2+}$  channels triggered by depolarization elicits a  $\text{Ca}^{2+}$  signal of varying spatial distribution.  $\text{Ca}^{2+}$  influx through channels at the fusion site create a local microdomain of elevated  $\text{Ca}^{2+}$ , which is thought to be highly effective in triggering membrane fusion (Neher, 1998). Complementing this view, the presence of a low-affinity  $\text{Ca}^{2+}$ -binding site at the active zone has been reported (Llinas et al., 1992a). Studies show that transmitter release at the presynaptic terminal is triggered by very well localized calcium concentration that may be as high as several hundred micromoles (Llinas et al., 1992b). Similarly, the release of transmitters from neurons requires  $\text{Ca}^{2+}$  concentration  $>100\text{ }\mu\text{M}$  (Mennerick and Matthews, 1996). Moreover, the  $\text{Ca}^{2+}$  increment within the microdomains will be strongly augmented in the presence of mobile buffer(s), or when  $\text{Ca}^{2+}$  influx occurs over regions of large clusters of densely packed  $\text{Ca}^{2+}$  channels (Neher, 1998). Contrariwise, a recent study shows that clusters of vesicles act as important diffusion barriers, and therefore can accumulate high  $\text{Ca}^{2+}$  concentrations at localized plasma membrane domains (Glavinovic and Rabie, 2001). The presence of  $200\text{ nm}$  vesicles, which are similar to the size of vesicles used in our study, for example, accumulates  $1.2\text{ mM}$  free  $\text{Ca}^{2+}$  within  $15\text{ nm}$  of the plasma membrane (Glavinovic and Rabie, 2001). With similar sensitivity ( $100\text{ }\mu\text{M}$  and higher),  $\text{Ca}^{2+}$  was found to elicit membrane fusion of artificial vesicles in our current

study. Furthermore, if lipid vesicles were to possess synaptotagmin or other  $\text{Ca}^{2+}$  sensors, they may further contribute to the increased sensitivity of  $\text{Ca}^{2+}$  on vesicles fusion.

## 5. Conclusion

We have demonstrated that t- and v-SNAREs, reconstituted into separate liposomes, modulate  $\text{Ca}^{2+}$  sensitivity of vesicle fusion. The presence of SNAREs in bilayers decreases the  $\text{Ca}^{2+}$  requirement for vesicle fusion and furthermore, and increases the overall yield of  $\text{Ca}^{2+}$ -induced fusion. Although SNAREs increases the potency of  $\text{Ca}^{2+}$ -induced fusion of lipid vesicles, it was not a requirement. In a complementary study with release-ready secretory vesicles from the sea urchin that recapitulates a functional, stage-specific physiological membrane preparation, neither presence nor disruption of the SNARE complex is essential to the  $\text{Ca}^{2+}$ -triggered fusion of these exocytotic membranes (Coorssen et al., 1998; Tahara et al., 1998). SNAREs serve as an anchor for membrane fusion by creating focal contact points between opposing bilayers (Cho et al., 2002d), which ensure the fusion to proceed in a highly regulatory fashion (Jena et al., 2002). A plethora of recent functional and structural studies (Hu et al., 2002; Kweon et al., 2003; Zimmerberg et al., 2000) including this study, demonstrates that SNARE complex obviously requires additional support to be considered efficient fusion machinery. The present study demonstrates  $\text{Ca}^{2+}$  to be this critical component in the fusion process.

Finally, as our experiments lacked synaptotagmin and other  $\text{Ca}^{2+}$  sensors by which  $\text{Ca}^{2+}$  can promote interaction between SNARE proteins on apposing membranes to initiate fusion (Chen et al., 1999; Lawrence and Dolly, 2002), we propose the  $\text{Ca}^{2+}$ -effect on membrane fusion to be direct. A proposed pathway would involve neutralization of the negatively charged phospholipid head groups by  $\text{Ca}^{2+}$ , resulting in enhanced membrane–membrane interactions and/or the formation of  $\text{Ca}^{2+}$ -phosphate bridges between opposing bilayers, freeing bilayers of interlamellar water, an important barrier for bilayer fusion.

## Acknowledgements

We thank Professor Milorad Jeremic, for critically reading the manuscript and for many helpful suggestions. This work is supported by NIH grants DK56212 and NS39918 to B.P.J. and NIH Postdoctoral Fellowship DK60368 to S.J.C.

## References

Beevers CA. *Acta Crystallogr D Biol Crystallogr* 1958;11:273–7.



- Chen YA, Scales SJ, Patel SM, Doung YC, Scheller RH. SNARE complex formation is triggered by  $\text{Ca}^{2+}$  and drives membrane fusion. *Cell* 1999;97:165–74.
- Chen YD, Rubin RJ, Szabo A. Fluorescence dequenching kinetics of single cell–cell fusion complexes. *Biophys J* 1993;65:325–33.
- Cho SJ, Jeftinija K, Glavaski A, Jeftinija S, Jena BP, Anderson LL. Structure and dynamics of the fusion pores in live GH-secreting cells revealed using atomic force microscopy. *Endocrinology* 2002a;143:1144–8.
- Cho SJ, Quinn AS, Stromer MH, Dash S, Cho J, Taatjes DJ et al. Structure and dynamics of the fusion pore in live cells. *Cell Biol Int* 2002b;26:35–42.
- Cho SJ, Sattar AK, Jeong EH, Satchi M, Cho JA, Dash S et al. Aquaporin 1 regulates GTP-induced rapid gating of water in secretory vesicles. *Proc Natl Acad Sci U S A* 2002c;99:4720–4.
- Cho SJ, Kelly M, Rognlien KT, Cho JA, Horber JK, Jena BP. SNAREs in opposing bilayers interact in a circular array to form conducting pores. *Biophys J* 2002d;83:2522–7.
- Coorsen JR, Blank PS, Tahara M, Zimmerberg J. Biochemical and functional studies of cortical vesicle fusion: the SNARE complex and  $\text{Ca}^{2+}$  sensitivity. *J Cell Biol* 1998;143:1845–57.
- Edwardson JM, An S, Jahn R. The secretory granule protein syncollin binds to syntaxin in a  $\text{Ca}^{2+}$ -sensitive manner. *Cell* 1997;90:325–33.
- Fasshauer D, Eliason WK, Brunger AT, Jahn R. Identification of a minimal core of the synaptic SNARE complex sufficient for reversible assembly and disassembly. *Biochemistry* 1998;37:10354–62.
- Glavinovic MI, Rabie HR. Monte Carlo evaluation of quantal analysis in the light of  $\text{Ca}^{2+}$  dynamics and the geometry of secretion. *Pflügers Arch* 2001;443:132–45.
- Hanson PI, Roth R, Morisaki H, Jahn R, Heuser JE. Structure and conformational changes in NSF and its membrane receptor complexes visualized by quick-freeze/deep-etch electron microscopy. *Cell* 1997;90:523–35.
- Hu K, Carroll J, Fedorovich S, Rickman C, Sukhodub A, Davletov B. Vesicular restriction of synaptobrevin suggests a role for calcium in membrane fusion. *Nature* 2002;415:646–50.
- Huster D, Paasche G, Dietrich U, Zschornig O, Gutberlet T, Gawrisch K et al. Investigation of phospholipid area compression induced by calcium-mediated dextran sulfate interaction. *Biophys J* 1999;77:879–87.
- Jahn R, Niemann H. Molecular mechanisms of clostridial neurotoxins. *Ann N Y Acad Sci* 1994;733:245–55.
- Jahn R, Sudhof TC. Membrane fusion and exocytosis. *Annu Rev Biochem* 1999;68:863–911.
- Jena BP, Cho SJ, Jeremic A, Stromer MH, Hamadah RA. Structure and composition of the fusion pore. *Biophys J* 2002;84:1337–43.
- Jeong EH, Webster P, Khuong CQ, Abdus Sattar AK, Satchi M, Jena BP. The native membrane fusion machinery in cells. *Cell Biol Int* 1998;22:657–70.
- Jeremic A, Kelly M, Cho SJ, Stromer MH, Jena BP. Reconstituted fusion pore. *Biophys J* 2003;85:2035–43.
- Kishimoto T, Liu TT, Ninomiya Y, Takagi H, Yoshioka T, Ellis-Davies GC et al. Ion selectivities of the  $\text{Ca}^{2+}$  sensors for exocytosis in rat pheochromocytoma cells. *J Physiol* 2001;533:627–37.
- Kulkarni K, Snyder DS, McIntosh TJ. Adhesion between cerebroside bilayers. *Biochemistry* 1999;38:15264–71.
- Kweon DH, Kim CS, Shin YK. Regulation of neuronal SNARE assembly by the membrane. *Nat Struct Biol* 2003;10:440–7.
- Laroche G, Dufourc EJ, Dufourcq J, Pezolet M. Structure and dynamics of dimyristoylphosphatidic acid/calcium complexes by  $^2\text{H}$  NMR, infrared, spectroscopies and small-angle x-ray diffraction. *Biochemistry* 1991;30:3105–14.
- Lawrence GW, Dolly JO.  $\text{Ca}^{2+}$ -induced changes in SNAREs and synaptotagmin I correlate with triggered exocytosis from chromaffin cells: insights gleaned into the signal transduction using trypsin and botulinum toxins. *J Cell Sci* 2002;115:2791–800.
- Llinas R, Sugimori M, Silver RB. Microdomains of high calcium concentration in a presynaptic terminal. *Science* 1992a;256:677–9.
- Llinas R, Sugimori M, Silver RB. Presynaptic calcium concentration microdomains and transmitter release. *J Physiol Paris* 1992b;86:135–8.
- MacDonald RC, MacDonald RI, Menco BP, Takeshita K, Subbarao NK, Hu LR. Small-volume extrusion apparatus for preparation of large, unilamellar vesicles. *Biochim Biophys Acta* 1991;1061:297–303.
- McIntosh TJ. Short-range interactions between lipid bilayers measured by X-ray diffraction. *Curr Opin Struct Biol* 2000;10:481–5.
- Mennerick S, Matthews G. Ultrafast exocytosis elicited by calcium current in synaptic terminals of retinal bipolar neurons. *Neuron* 1996;17:1241–9.
- Nagle JF, Tristram-Nagle S. Structure of lipid bilayers. *Biochim Biophys Acta* 2000;1469:159–95.
- Neher E. Vesicle pools and  $\text{Ca}^{2+}$  microdomains: new tools for understanding their roles in neurotransmitter release. *Neuron* 1998;20:389–99.
- Newton C, Pangborn W, Nir S, Papahadjopoulos D. Specificity of  $\text{Ca}^{2+}$  and  $\text{Mg}^{2+}$  binding to phosphatidylserine vesicles and resultant phase changes of bilayer membrane structure. *Biochim Biophys Acta* 1978;506:281–7.
- Ohki S. A mechanism of divalent ion-induced phosphatidylserine membrane fusion. *Biochim Biophys Acta* 1982;689:1–11.
- Ohki S. Effects of divalent cations, temperature, osmotic pressure gradient, and vesicle curvature on phosphatidylserine vesicle fusion. *J Membr Biol* 1984;77:265–75.
- Parlati F, Weber T, McNew JA, Westermann B, Sollner TH, Rothman JE. Rapid and efficient fusion of phospholipid vesicles by the  $\alpha$ -helical core of a SNARE complex in the absence of an N-terminal regulatory domain. *Proc Natl Acad Sci U S A* 1999;96:12565–70.
- Parsons TD, Coorsen JR, Horstmann H, Almers W. Docked granules, the exocytic burst, and the need for ATP hydrolysis in endocrine cells. *Neuron* 1995;15:1085–96.
- Pauling L, Corey RB. A proposed structure for the nucleic acids. *Proc Natl Acad Sci U S A* 1953;39:84–97.
- Plattner H, Artalejo AR, Neher E. Ultrastructural organization of bovine chromaffin cell cortex-analysis by cryofixation and morphometry of aspects pertinent to exocytosis. *J Cell Biol* 1997;139:1709–17.
- Poirier MA, Hao JC, Malkus PN, Chan C, Moore MF, King DS et al. Protease resistance of syntaxin.SNAP-25.VAMP complexes. Implications for assembly and structure. *J Biol Chem* 1998;273:11370–7.
- Portis A, Newton C, Pangborn W, Papahadjopoulos D. Studies on the mechanism of membrane fusion: evidence for an intermembrane  $\text{Ca}^{2+}$ -phospholipid complex, synergism with  $\text{Mg}^{2+}$ , and inhibition by spectrin. *Biochemistry* 1979;18:780–90.
- Sattar AA, Boinpally R, Stromer MH, Jena BP.  $\text{Gal}\alpha(13)$  in Pancreatic Zymogen Granules Participates in Vesicular Fusion. *J Biochem (Tokyo)* 2002;131:815–20.
- Schneider SW, Sritharan KC, Geibel JP, Oberleithner H, Jena BP. Surface dynamics in living acinar cells imaged by atomic force microscopy: identification of plasma membrane structures involved in exocytosis. *Proc Natl Acad Sci U S A* 1997;94:316–21.
- Shannon RD. *Acta Crystallogr D Biol Crystallogr* 1976;A32:751.
- Sheng ZH, Rettig J, Cook T, Catterall WA. Calcium-dependent interaction of N-type calcium channels with the synaptic core complex. *Nature* 1996;379:451–4.
- Sollner T, Whiteheart SW, Brunner M, Erdjument-Bromage H, Geromanos S, Tempst P et al. SNAP receptors implicated in vesicle targeting and fusion. *Nature* 1993;362:318–24.



- Sudhof TC, Rizo J. Synaptotagmins: C2-domain proteins that regulate membrane traffic. *Neuron* 1996;17:379–88.
- Tahara M, Coorssen JR, Timmers K, Blank PS, Whalley T, Scheller R et al. Calcium can disrupt the SNARE protein complex on sea urchin egg secretory vesicles without irreversibly blocking fusion. *J Biol Chem* 1998;273:33667–73.
- Weber T, Zemelman BV, McNew JA, Westermann B, Gmachl M, Parlati F et al. SNAREpins: minimal machinery for membrane fusion. *Cell* 1998;92:759–72.
- Wilschut J, Duzgunes N, Fraley R, Papahadjopoulos D. Studies on the mechanism of membrane fusion: kinetics of calcium ion induced fusion of phosphatidylserine vesicles followed by a new assay for mixing of aqueous vesicle contents. *Biochemistry* 1980;19:6011–21.
- Wilschut J, Duzgunes N, Papahadjopoulos D. Calcium/magnesium specificity in membrane fusion: kinetics of aggregation and fusion of phosphatidylserine vesicles and the role of bilayer curvature. *Biochemistry* 1981;20:3126–33.
- Zimmerberg J, Blank PS, Kolosova I, Cho MS, Tahara M, Coorssen JR. A stage-specific preparation to study the Ca(2+)-triggered fusion steps of exocytosis: rationale and perspectives. *Biochimie* 2000;82:303–14.